Critical state in finite type-II superconducting rings

C. Navau,[1,2] A. Sanchez,[1] E. Pardo,[1] D.-X. Chen,[3,1] E. Bartolomé,[4] X. Granados,[4] T. Puig,[4] and X. Obradors[4]
[1]*Grup d'Electromagnetisme, Departament de Física, Universitat Autònoma de Barcelona, 08193 Bellaterra, Barcelona, Catalonia, Spain*
[2]*Escola Universitària Salesiana de Sarrià, Pg. Sant Joan Bosco 74, 08017 Barcelona, Catalonia, Spain*
[3]*Institució Catalana de Recerca i Estudis Avançats (ICREA), Campus UAB, 08193 Bellaterra, Barcelona, Catalonia, Spain*
[4]*Institut de Ciència de Materials de Barcelona (ICMAB), Campus UAB, 08193 Bellaterra, Barcelona, Catalonia, Spain*
(Received 23 November 2004; published 6 June 2005)

We study the magnetic behavior of a finite superconducting ring in the presence of a uniform applied field directed along its axis by means of the critical-state model and the minimization of magnetic energy. We systematically study the dependence of the magnetization and the ac susceptibility upon the geometry of the ring and develop an approximate analytical expression for the case of narrow rings of any aspect ratio. Besides, we show how the critical-current density of the superconductor can be obtained from magnetization measurements and conclude that ring geometry is a very convenient one for such a purpose. In particular, we present an expression for the full penetration field in the case of finite rings, which allows us to find the value of the critical current from the value of the magnetic field at just one point on the axis of the ring.

DOI: 10.1103/PhysRevB.71.214507 PACS number(s): 74.25.Sv, 74.25.Ha, 74.78.−w, 74.72.Bk

I. INTRODUCTION

The macroscopic magnetic properties of type-II superconductors depend on the value of its critical-current density, J_c, which is often experimentally obtained from magnetization measurements of the superconductors, normally by using Bean's critical-state model.[1] Since the relation between J_c and the magnetization data depends strongly on geometry, it is very convenient to explore different superconductor geometries in order to optimize a process for accurately obtaining J_c.

In the critical-state model framework, the dependence of the critical current upon the internal field, $J_c(H_i)$, is commonly obtained from the width of the measured magnetization loop, divided by some characteristic length of the sample, $J_c=\Delta M(H_a)/d$. This method was originally derived for the case of J_c independent of H_i (Bean's model). If, instead, J_c depends on the internal field, what is obtained is a function $J_c(H_a)$ which is, in principle, not exactly the intrinsic dependence of the critical current with the internal field function, $J_c(H_i)$. These two functions are approximately equal only if some conditions concerning the internal field homogeneity are met.[2–6] It has been demonstrated that the superconducting critical current density and its dependence on the internal field can be more precisely obtained from the magnetization loops when measuring thin samples in perpendicular applied magnetic fields up to sufficiently high applied fields, because in this case demagnetization fields help create most adequate conditions for extracting $J_c(H_i)$.[6]

An important parameter involved in the determination of J_c from magnetic measurements is the full penetration field, H_{pen}. This field, defined as the minimum applied field at which a zero-field cooled type-II superconductor becomes fully penetrated on the initial magnetization curve, is related to the critical-current density and to the geometry of the sample. In the simplest case of constant J_c, $H_{pen}=J_c f(\Omega)$, where $f(\Omega)$ represents a function of only the geometry of the sample. If $f(\Omega)$ can be theoretically found, J_c can be simply extracted from the measurement of H_{pen} which, sometimes, can be obtained from techniques such as Hall probe measurements.[7]

The full penetration field for the case of constant J_c can be analytically obtained in general whenever the last penetrated point, P, after an increase of the applied field from zero, is known. In these cases, H_{pen} equals the magnetic field created by currents in the penetrated sample at P.[8] In this way, analytical expressions for finite cylinders,[8] tapes of finite cross section,[9] and multifilamentary tapes[9] have been derived. In other geometries, the full penetration field has been obtained by using a numerical procedure for calculating the complete current penetration process.[10–12] A similar procedure for finding the full penetration field of finite cylinders for the case of J_c depending on the internal field was presented in Ref. 10. Of special relevance is the fact that for very thin samples the field of full penetration is of the order of $J_c d$ where d is the short dimension of the sample, not of $J_c a$, being a the large dimension.[13]

In this paper we will focus on the ring geometry. The practical importance of finite cylinders and rings comes from their use as key components in devices such as magnetic bearings[14] or as permanent magnets.[15] The ring geometry has also been used to study grain boundaries in melt-textured superconductors.[16,17] The ring geometry maintains the cylindrical symmetry but, because of the inner hole, presents some properties different from those of a bulk cylindrical superconductor. In particular, the ring shape geometry can have a lower ratio of weight to trapped magnetic flux than a cylindrical bulk superconductor.[18] Furthermore, since the stress is the largest at the center of a disk, in a ring sample, one can avoid some mechanical problems by removing this central part of the superconductor.[19] Finally, we shall demonstrate in this work that the ring geometry presents some characteristics that make it an optimum geometry for the determination of J_c from magnetic measurements.

 ©2005 The American Physical Society

Although the ring geometry is a particular case of cylindrically symmetric systems, no detailed study of current penetration, magnetization loops, and susceptibility has been reported for the case of a finite ring. Only partial results are known until now, summarized as follows. The full penetration field for infinitely long rings is $H_{\text{pen}}^{\infty\text{-ring}}=J_c(R_{\text{out}}-R_{\text{int}})$, where R_{int} is the interior radius of the ring and R_{out} is the external radius of the ring, whereas on the other limit, an approximate expression for the field of full penetration of thin rings can be found in Ref. 20 (see below). As far as we know, neither expressions nor numerical results for the penetration field in the general case of a finite superconducting ring have been reported.

In this work we will present a systematic study of the magnetic behavior of a superconducting finite ring in the presence of an applied field directed along its principal axis. The paper is structured as follows. In Sec. II, we discuss the main properties of the penetration of currents inside the superconducting ring, the way to calculate the full penetration field and how to obtain the critical current of the superconductor from field measurements. We will illustrate the method with an application of the procedure to an actual measurement of a $Y_1Ba_2Cu_3O_7$ superconducting ring. In Sec. III, we calculate and discuss the magnetization and susceptibility of the rings, including an analytical model for narrow rings, and how they can be used to measure the full penetration field. Finally, the conclusions are presented in the last section.

II. CURRENT PROFILES AND FULL PENETRATION FIELD

A. Model

We consider a type-II superconducting ring of axial length L, inner radius R_{int}, and external radius R_{out}. We use cylindrical coordinates with the origin located at the geometrical center of the ring and the z axis along its axis.

We assume a uniform applied field, $\mathbf{H}_a=H_a\hat{\mathbf{z}}$, and that the superconductor obeys the critical-state model,[1] with a constant critical-current density, J_c. We also assume that there are neither equilibrium magnetization nor surface barriers in the superconductor, which is equivalent to consider applied fields much larger than the lower critical field, H_{c1}.

In this work we will calculate the current distribution for a given H_a following the energy minimization numerical procedure presented in Refs. 10,21. We give a brief overview of the process as follows.

We start with a zero-field cooled superconductor. Due to the cylindrical symmetry, any induced current will flow in angular direction $\mathbf{J}=J_\theta(\rho,z)\hat{\theta}$. We discretize the superconductor as a set of $n\times m$ coaxial circuits (rings) of rectangular cross section and define $\Delta R=R/n$ and $\Delta L=L/m$. Setting a current I_{ij} at a circuit indexed as ij requires an energy $E_{ij}=\frac{1}{2}L_{ij}I_{ij}^2$, (where L_{ij} is the self-inductance of the ij circuit) while it contributes to reduce the energy by a factor $I_{ij}\phi_{ij}^{ext}$, where $\phi_{ij}^{ext}=\mu_0 H_a \pi\rho_i^2$ is the magnetic flux threading the circuit i, which has a radius ρ_i. We find in this way the circuit that yields the largest decrease of energy and set a current I there. Following the Bean's critical state model we put a current with value $I=J_c(\Delta R)(\Delta L)$, for a given J_c value. When there are other currents already set in the superconductor there exists an extra contribution to the magnetic energy coming from the mutual inductances of all present currents

$$E_{ij}=\left(\sum_{kl\neq ij} M_{ij,kl}I_{kl}\right)I_{ij}. \tag{1}$$

The calculation of self and mutual inductances is described in Ref. 10.

This process is repeated until it becomes impossible to decrease the magnetic energy by setting a new current anywhere. Then, from the existing current profiles one can calculate the corresponding magnetization (Sec. III A). When the field is further increased, the same procedure starts again from the previous current values.

The described procedure solves numerically the critical-state problem in cylindrically symmetric cases (even if the applied field is not uniform).[22,23] This model has also been developed for the case of J_c depending on the internal field[10] and has been applied to the study the critical state penetration in other geometries such as multifilamentary tapes.[9] In general, the procedure allows us to calculate current profiles as long as the direction of the induced currents is known. It is clear that in the case of rings with an axial applied field, the induced currents must always flow in the azimuthal direction.

In order to present a systematic analysis, we normalize the lengths to R_{out} and the magnetic quantities to J_cR_{out}, so that the results only depend on dimensionless ratios $\gamma=L/R_{\text{out}}$ and $\delta=R_{\text{int}}/R_{\text{out}}$, and not on the particular values of J_c, R_{int}, or R_{out}. The quantity J_cR_{out} is the full penetration field of an infinitely long bulk cylinder: $H_{\text{pen}}(\gamma\to\infty,\delta=0)=J_cR_{\text{out}}$.

B. Current and field profiles

In Fig. 1 we show the calculated current penetration profiles for several zero-field cooled rings with different values of γ and δ. We plot three sets of figures corresponding to cases of $\gamma=5.0$, 1, and 0.2. For every case we consider $\delta=0.8$, 0.5, and 0.2, and, for comparison, $\delta=0$, which corresponds to the case of a bulk cylinder. In all cases we show the current profiles at applied fields starting from zero and increased in increments of 0.1 J_cR_{out} (J_c is assumed the same for all samples). It can be observed the expected behavior due to the demagnetization effects: there is a large penetration in the upper and lower faces of the rings and a deeper penetration from the lateral surface for lower-γ rings.[10,24]

It is known that for an infinite superconducting ring (a tube) the induced critical current shields the applied field not only in its interior but also in the hole before it reaches the saturation. In the present case of finite superconducting rings, the field in the hole is not null, and induced currents tend to shield the superconductor volume but not the hole. An interesting property is that the total magnetic flux that passes through a circle on the $z=0$ plane in the core of the superconductor (the region which is not penetrated by currents) is zero, as can be demonstrated by calculating the circulation of the vector potential along a circle in the core.

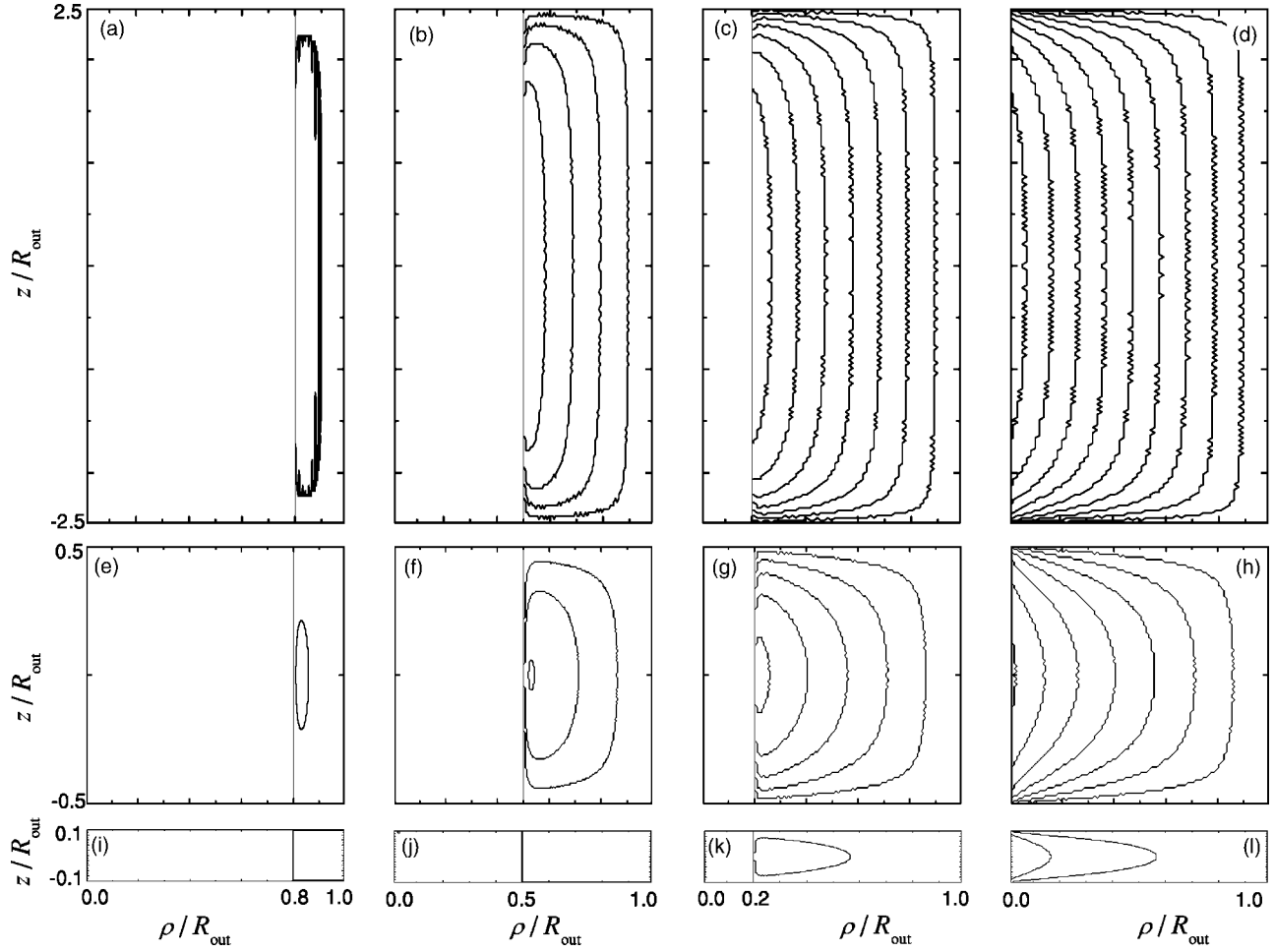

FIG. 1. Calculated penetration profiles for twelve rings at different applied fields. Upper line (a)-(b)-(c)-(d): $\gamma=5$, center line (e)-(f)-(g)-(h): $\gamma=1.0$, and bottom line (i)-(j)-(k)-(l): $\gamma=0.2$. Left column (a)-(e)-(i): $\delta=0.8$, center left column (b)-(f)-(j): $\delta=0.5$, center right column (c)-(g)-(k): $\delta=0.2$, and right column (d)-(h)-(l): $\delta=0$ (bulk cylinder). In all cases, the applied field H_a increases from zero in steps of $\Delta H_a=0.1J_cR_{out}$. Only a semiplane of constant angle is plotted. In each figure, the left axis corresponds to the rotation axis. The length dimensions in the $\gamma=5$ sample have been reduced by a factor of 2.5.

Since some field passes through the hole, in the inner surface region of the finite ring there should be some current (see Fig. 2). However, for a given applied field that does not produce a full penetration, the presence of the hole slightly modifies the general profile formed by the currents. We show in Fig. 1 that the penetration from the inner surface is very shallow, except for larger δ and lower γ (due to numerical precision in the calculations the narrow penetration from the hole is not seen in some of the cases in Fig. 1). In other words, although there is always penetration from the inner surface, currents penetrate mainly from the external surface to inside the superconductor. The presence of the hole basically marks the ends of the superconducting region and produces slight variation in the penetration profile. The full penetration field will therefore be, for a given γ, lower for larger δ mainly because the superconducting region is smaller.

For narrow rings ($\delta\simeq 1$), specially if they are short, the last penetration place is significatively far from the inner surface. To see more clearly this effect we show in Fig. 2 the magnetic field lines[25] for the case $\gamma=0.2$, $\delta=0.8$ at different values of the applied field. We observe as many closed lines (around the superconducting region) as lines passing through the hole, confirming that the total flux passing through a circle in the core of the superconductor is zero.

C. Full penetration field

Since current penetrates in the rings not only from the outer surfaces but also from the inner one, the last penetrated place in a superconducting ring is, in general, unknown. From the symmetry of the problem one can only ensure that the last penetrated place lies on the midplane ($z=0$) of the ring, but cannot know where exactly it is. Thus, it is impossible to find the analytical solution for the penetration field following the method of calculating the field created by the fully penetrated sample at the last penetrated point.[8]

However, we can use the energy minimization procedure to numerically obtain the penetration field as the applied field at which the last place becomes penetrated by currents. Calculated results are presented in Fig. 3, where we have plotted the calculated penetration field (normalized to J_cR_{out}) as a function of γ for different δ values. We observe in the figure

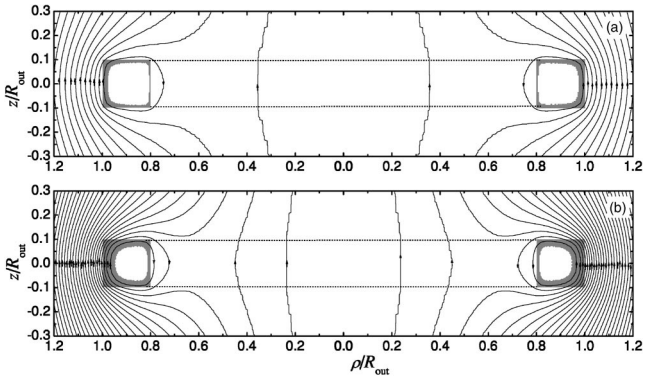

FIG. 2. Approximate field lines for a ring with $\gamma=0.2$ and $\delta=0.8$. Applied fields are (a) $H_a/J_cR_{out}=0.1$ and (b) 0.02. Gray regions correspond to current penetrated regions.

that the full penetration field increases with increasing γ for all δ's. This is because, for a fixed δ, a larger γ means a smaller demagnetizing effect so that the increment of the internal field inside the superconductor due to demagnetization is smaller. As a consequence, the full penetration of the sample is achieved at larger applied fields (the detailed explanation is similar to that for bulk finite cylinders; see, for example, Ref. 10).

For the general case of arbitrary γ and δ, we propose an approximate expression for $H_{pen}(\gamma,\delta)$:

$$\frac{H_{pen}(\gamma,\delta)}{J_cR_{out}}=\frac{\gamma}{2}\frac{(1-\delta)}{(1+\delta)}\ln\left(\frac{2(1+\delta)}{\gamma}+\left\{1+\left[\frac{2(1+\delta)}{\gamma}\right]^2\right\}^{1/2}\right). \tag{2}$$

This equation contains the known analytical limits for long samples and bulk cylinders. In the limit $\gamma\to\infty$, there are no demagnetization effects and the full penetration field, $H_{pen}(\gamma\to\infty,\delta)=H_{pen}^{\infty\text{-ring}}$ tends to

$$\frac{H_{pen}^{\infty\text{-ring}}}{J_cR_{out}}=1-\delta. \tag{3}$$

In the case of bulk cylinders, the full penetration field, $H_{pen}(\gamma,\delta=0)=H_{pen}^{cyl}$, is

$$\frac{H_{pen}^{cyl}}{J_cR_{out}}=\frac{\gamma}{2}\ln\left\{\frac{2}{\gamma}+\left[1+\left(\frac{2}{\gamma}\right)^2\right]^{1/2}\right\}, \tag{4}$$

which is the expression analytically obtained by Forkl[8] for the case of finite cylinders.

When $\gamma\ll 1$, Eq. (2) reduces to

$$\frac{H_{pen}(\gamma\ll 1,\delta)}{J_cR_{out}}=\frac{\gamma}{2}\frac{(1-\delta)}{(1+\delta)}\ln\left[\frac{4(1+\delta)}{\gamma}\right]. \tag{5}$$

For very thin superconducting rings, another approximate expression was presented[20] for the full penetration field, $H_{pen}^{thin\text{-}ring}$,

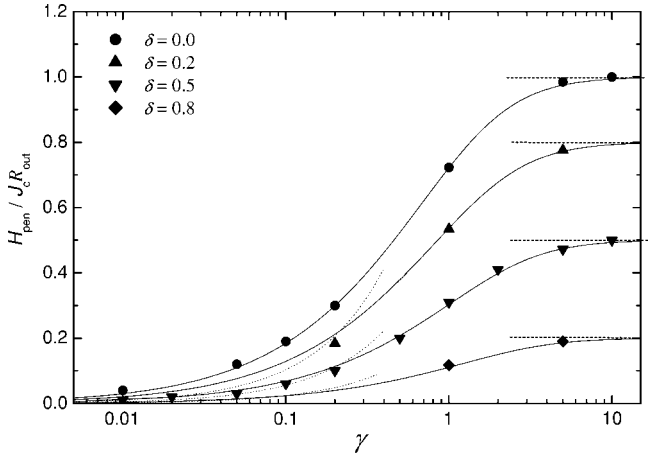

FIG. 3. Calculated penetration field for different δ values as a function of γ. The different symbols correspond to the numerically calculated penetration field (see text) for different δ's. Solid lines correspond to the approximate expression of Eq. (2). Dotted lines correspond to the approximation for thin ring [Eq. (6)] whereas dashed lines correspond to the infinite ring limit [Eq. (3)].

$$\frac{H_{pen}^{thin\text{-}ring}}{J_cR_{out}}=\gamma\left(\frac{2}{\pi}\frac{(1-\delta)}{(1+\delta)}\left\{\ln\left[\frac{8(1+\delta)}{(1-\delta)}\right]-1\right\}-\frac{1}{2}(\ln\delta+1-\delta)\right), \tag{6}$$

where the induced current is considered as the average of the current across the L dimension. This yields a full penetration field just proportional to L for very small γ's.

We have included in Fig. 3 the approximate expression of Eq. (2) and the limiting cases of infinitely long rings [Eq. (3)] and thin rings [Eq. (6)] for comparison.

D. Determination of J_c from direct Hall-probe measurements

Several methods for experimentally obtaining J_c are based on the measurement of the full penetration field together with the use of an expression that relates this field with J_c. For example, for a thin ring geometry, Pannetier *et al.*[7] found that the (z component of the) magnetic field measured above the superconductor has a minimum at the radial distance corresponding to the inner radius for a given current penetration. They argued that this minimum was the largest (in absolute value) just when the applied field equaled the full penetration field. This procedure, accurate for thin rings, would fail for larger γ because the minimum of the field above the superconductor does not always accomplish the above condition.

We propose an alternative method to measure H_{pen}, and thus J_c, from the measurement of the magnetic field at just one point. In Fig. 4 we show the calculated magnetic field on the axis of the ring at the point just above the superconducting ring surface ($\rho=0, z=L/2$) as a function of the (uniform) applied field. We have plotted the results for two rings with $\delta=0.5$ and 0.8, with three different γ's for each case. One can observe a kink just at the value of the full penetration field. This kink is more evident, and therefore H_{pen} is more easily measured, as the superconducting ring becomes thin-

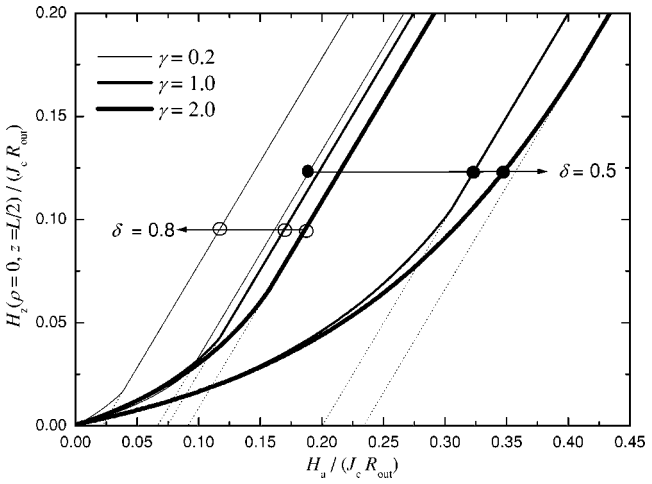

FIG. 4. (a) Calculated z component of the magnetic field at the center of the top surface of the ring ($z=L/2, \rho=0$) as a function of the applied field. Different lines correspond to different rings: from thinner to thicker line $\gamma=0.2$, 1.0, and 2.0. The lines marked with open and solid symbols correspond to $\delta=0.8$ and 0.5, respectively. The dotted lines correspond to the field created by fully penetrated rings (analytically calculated). They provide an easy visualization of the kink in each curve (see text).

ner, narrower, and when measuring the field as close to the geometrical center ($z=0;\rho=0$) of the ring as possible. The ring geometry becomes, thus, an optimum geometry to measure the critical current of the superconducting material.

When the applied field is lower than the penetration field, the total field at the chosen point depends on the current penetrated region and can be only numerically calculated (as in Fig. 4). Only when the superconductor is fully penetrated the total field at point ($\rho=0, z=L/2$) can be analytically calculated as

$$\frac{H_z(\rho=0,z)}{J_c R_{\text{out}}} = \frac{H_a}{J_c R_{\text{out}}} + \frac{L}{2R_{\text{out}}}\left[\ln\frac{R_{\text{out}}+\sqrt{(z-L/2)^2+R_{\text{out}}^2}}{R_{\text{int}}+\sqrt{(z-L/2)^2+R_{\text{int}}^2}} - \ln\frac{R_{\text{out}}+\sqrt{(z+L/2)^2+R_{\text{out}}^2}}{R_{\text{int}}+\sqrt{(z+L/2)^2+R_{\text{int}}^2}}\right]. \quad (7)$$

Once the full penetration field is known, the use of Eq. (2) will allow us to find the critical current density of the superconductor. In practice, the full penetration field can be more clearly determined if plotting derivatives of the z-component of the total field at point ($\rho=0, z=L/2$) with respect to the applied field.

In order to illustrate the validity of this approach we have made an experiment with an $Y_1Ba_2Cu_3O_7$ ring[26,27] of dimensions $R_{\text{out}}=2.45$ mm, $R_{\text{int}}=1.63$ mm, $L=0.17$ mm. We have measured the magnetic field with a Hall probe located on the axis of the ring and at a distance $d\simeq 80$ μm above the top face of the ring. The ring was initially zero-field cooled and then an applied field was applied parallel to the ring axis, which was also the c axis of the superconductor. In Fig. 5 we present the measured values of the field together with the second derivative of the data with respect to the applied field (calculated by standard numerical derivation procedures). We

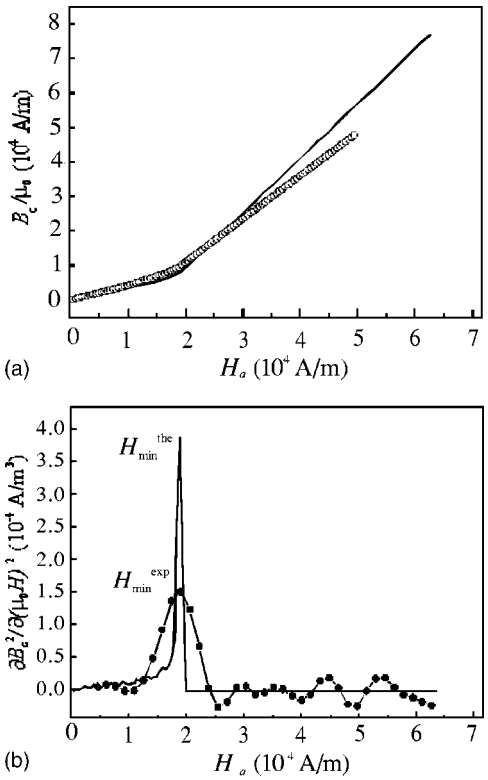

FIG. 5. Experimental and calculated (a) magnetic field and (b) its second derivative as a function of the applied field at the point $z=L/2$, $\rho=0$. Points correspond to experimental data and solid curves to calculated data.

observe the presence of a kink in the field data which corresponds to an appreciable peak in the second derivative. This peak gives the value of the measured penetration field of the ring. We have obtained in this way $H_{\text{pen}}^{\text{exp}}\approx 1.9\times 10^4$A/m. With the dimensions of the ring and the measured $H_{\text{pen}}^{\text{exp}}$ we find the value $J_c^{\text{exp}}\approx 4.0\times 10^8$A/m^2 using the numerically calculated H_{pen} [we could have as well used Eq. (1), with slightly less accuracy]. In order to check the consistency of the method we also plot the calculated data by inserting in the calculations this value of the critical current. As expected, the kink in the total applied field, as well as the maximum in the second derivative coincide with the experimentally observed. The main difference is that in the calculated data the kink is more prominent.

This is a simple outline of the procedure we can use for measuring the critical-current density in a superconductor, assumed as constant. One of the sources of imprecision in this procedure comes from the smoothness in the second derivative peak and in the accuracy in which this derivative can be obtained. A large number of points in the raw data curve and a closer position of the Hall probe to the center of the ring can yield a better precision, since the kink would be more evident. Another source of inaccuracy comes from the approximation in Eq. (2). Whenever high accuracy is required and other error sources have been minimized, one can use the numerically calculated values instead of the approximated formula.

However, in most of the cases, the consideration of the constant critical-current density becomes the main source of

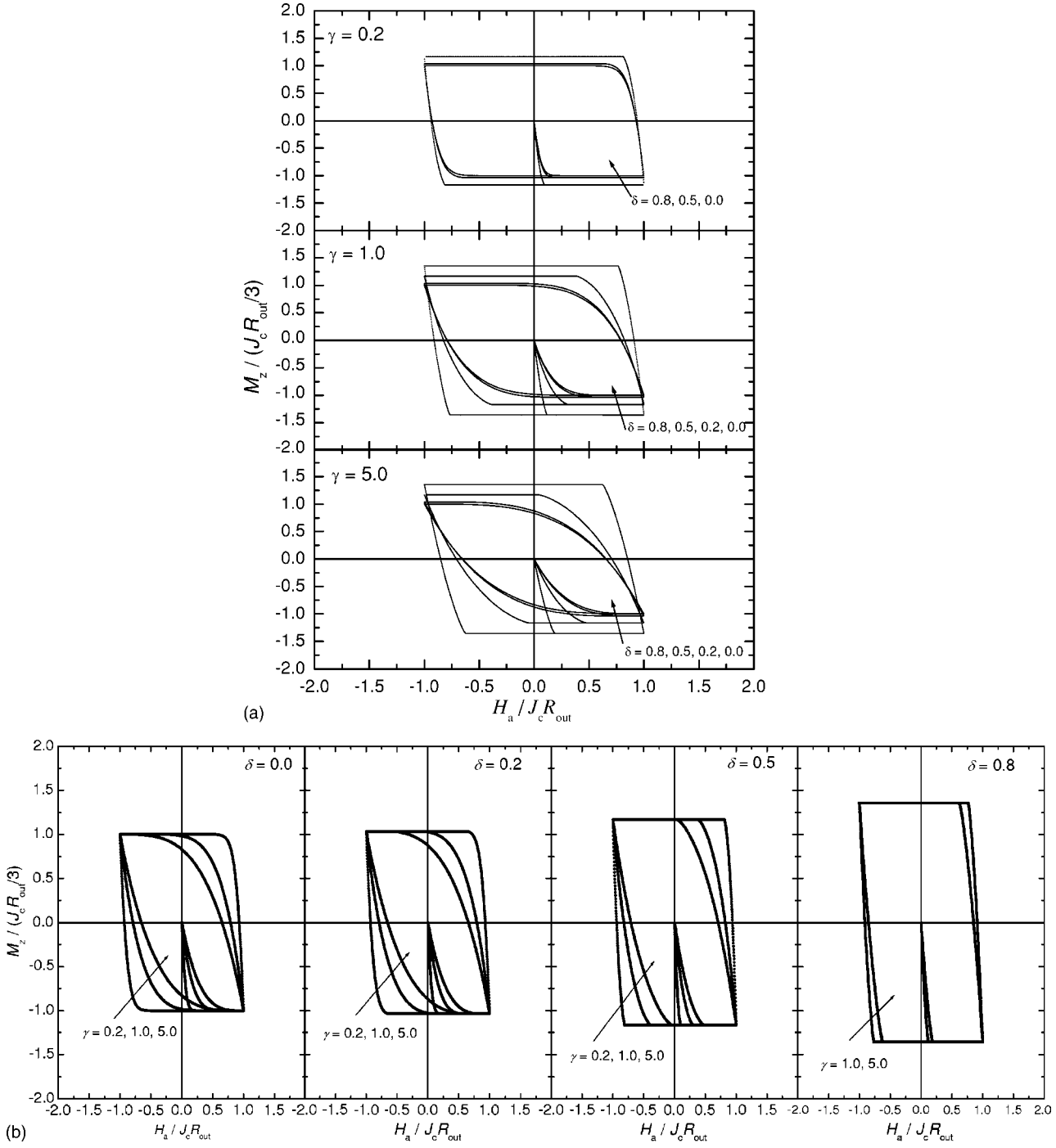

FIG. 6. Calculated magnetization loops for different rings. (a) Results for fixed γ and different δ [δ=0.0 (inmost), 0.2, 0.5, and 0.8 (outmost)]. (b) Results for fixed δ and different γ [γ=5 (inner), 1, 0.2 (outer)].

experimental error. A more detailed procedure for obtaining the $J_c(H_i)$ dependence will be published elsewhere. In the present example, provided that the sample has a small γ, the dependence on the internal field is weak in the range of fields used and this makes the procedure work well. In general, this method would be applicable when γ is small and when the dependence of the critical current density upon the internal field is not very strong.

III. MAGNETIZATION LOOPS AND SUSCEPTIBILITY

A. General expressions

Once the current penetration process is known, the magnetization and the ac susceptibility can be calculated as a function of the applied field. We define the magnetization as the magnetic moment per unit volume of superconducting material. In the present case, the magnetization will have only z component given by

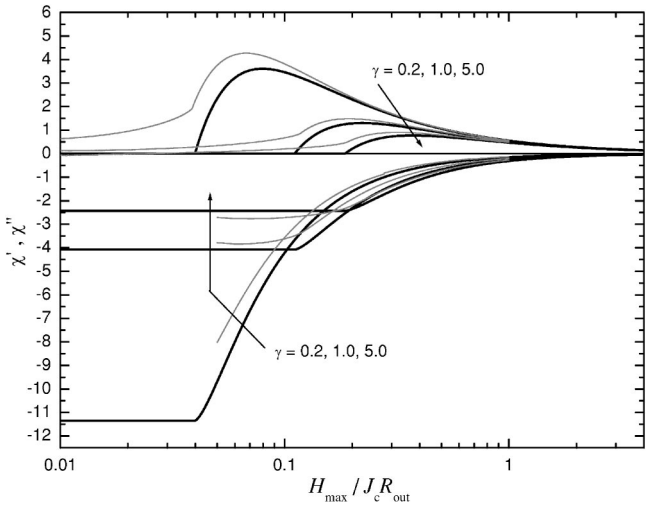

FIG. 7. Calculated real and imaginary susceptibility and modeled susceptibility Eqs. (23) and (25) as a function of the ac field amplitude.

$$M_z = \frac{J_c}{(R_{\text{out}}^2 - R_{\text{int}}^2)L}\int_\Omega \rho' \mathrm{d}\rho' \mathrm{d}z, \tag{8}$$

where Ω represents the current penetrated region. When the sample is fully penetrated by currents, Ω is the entire volume of the superconductor and the magnetization achieves its maximum (in magnitude) saturated value, given by

$$\frac{M_{\text{sat}}}{J_c R_{\text{out}}} = \frac{1}{3}\left(1 + \frac{\delta^2}{1+\delta}\right). \tag{9}$$

We note that the saturation magnetization is independent of γ but depends on δ. The magnetic moment of a ring in the fully penetrated state can be considered as that of a cylinder of radius R_{out} after subtracting that of another cylinder of radius R_{int}. Since $J_c R_{\text{out}}/3$ corresponds to the saturation magnetization of a bulk cylinder (either thin,[28] finite,[10] or infinitely long[1]), and the factor $1+\delta^2/(1+\delta)$ is always larger than unity, we note that the saturated magnetization for a ring is always larger than that of the cylinder with the same γ. It is also interesting to note that, for a very narrow ring ($\delta \to 1$), the saturation magnetization tends to $J_c R_{\text{out}}/2$.

Since J_c is constant, the complete magnetization loop can be calculated from the virgin magnetization curve as[28]

$$M_{\text{rev}}(H_a) = M_{\text{ini}}(H_0) - 2M_{\text{ini}}\left(\frac{H_a - H_0}{2}\right), \tag{10}$$

$$M_{\text{ret}}(H_a) = -M_{\text{rev}}(-H_a), \tag{11}$$

where H_0 is the maximum applied field after a zero-field cooling process, M_{ini} represents the initial virgin magnetization (applied field from 0 to H_0), $M_{\text{rev}}(H_a)$ is the reversal curve (applied field from H_0 to $-H_0$), and $M_{\text{ret}}(H_a)$ is the returning curve (applied field from $-H_0$ to H_0).

The ac susceptibility can be calculated from the magnetization loops. Defining the complex susceptibility as $\chi = \chi' - i\chi''$, the real and imaginary susceptibility (first harmonic component) for an ac applied field in the form $H_a = H_0\cos(\theta)$ can be calculated as[28]

$$\chi' = \frac{2}{\pi H_0}\int_0^\pi M_{\text{rev}}[H_a(\theta)]\cos(\theta)d\theta, \tag{12}$$

$$\chi'' = \frac{2}{\pi H_0}\int_0^\pi M_{\text{rev}}[H_a(\theta)]\sin(\theta)d\theta. \tag{13}$$

For the case of constant J_c, these expressions can be evaluated directly from the virgin magnetization curve (which, from the simulation point of view has the advantage of reducing considerably the computation time). In that case the susceptibilities can be calculated as

$$\chi'(H_0) = \frac{-8}{\pi H_0^2}\int_0^{H_0} M_{\text{ini}}(H')\frac{H_0 - 2H'}{\sqrt{H_0^2 - (H_0 - 2H')^2}}dH', \tag{14}$$

$$\chi''(H_0) = \frac{4}{\pi H_0^2}\left[M_{\text{ini}}(H_0)H_0 - 2\int_0^{H_0} M_{\text{ini}}(H')dH'\right]. \tag{15}$$

As a general fact of the critical state with constant J_c, both χ' and χ'' for fields above H_{pen} can be calculated directly just from their values at H_{pen} and the saturation magnetization. From Eqs. (14) and (15) we find

$$\chi'(H_0 \geqslant H_{\text{pen}}) = \chi'(H_{\text{pen}}) + \frac{8}{\pi H_0^2}M_{\text{sat}}\sqrt{\frac{H_{\text{pen}}}{H_0} - \left(1 - \frac{H_{\text{pen}}}{H_0}\right)}, \tag{16}$$

$$\chi''(H_0 \geqslant H_{\text{pen}}) = \chi''(H_{\text{pen}})\frac{H_{\text{pen}}^2}{H_0^2} + \frac{4M_{\text{sat}}(H_{\text{pen}} - H_0)}{\pi H_0^2}. \tag{17}$$

In particular, these equations are valid for H_0 larger than $J_c R_{\text{out}}$ for all δ and γ values, since this is the largest value for the full penetration field [$H_{\text{pen}}(\gamma, x) \leqslant J_c R_{\text{out}}$; see Fig 3]. The analytical expressions for M_{sat} and H_{pen} are given in Eqs. (2) and (9), respectively.

B. Analytical model for narrow rings

In the cases in which the maximum applied field is much larger than the penetration field, we have observed that the virgin magnetization curve can be rather well described by two straight lines. This condition is well fulfilled in the case of narrow rings of any value of γ. In general, the thinner the sample is, the better the condition is fulfilled.

We introduce in this section a simple model to analytically obtain the magnetization and susceptibility for narrow rings. A similar model was already proposed for very thin

and narrow rings.[29] Here we extend it to the case of narrow rings with any γ value.

We approximate the initial magnetization by the two following straight lines:

$$M_{\mathrm{ini}}(H_{\mathrm{a}}) = \frac{M_{\mathrm{sat}} H_{\mathrm{a}}}{H_{\mathrm{pen}}} \quad 0 < H_{\mathrm{a}} \leqslant H_{\mathrm{pen}}, \tag{18}$$

$$M_{\mathrm{ini}}(H_{\mathrm{a}}) = M_{\mathrm{sat}} \quad 0 < H_{\mathrm{pen}} \leqslant H_{\mathrm{a}}, \tag{19}$$

where H_{pen} and M_{sat} are given by Eqs. (2) and (9), respectively.

The reversal and the returning curves are obtained directly from the initial virgin curve using Eq. (10). We must distinguish two cases, $H_0 < H_{\mathrm{pen}}$ and $H_0 > H_{\mathrm{pen}}$: (a) When $H_0 < H_{\mathrm{pen}}$,

$$M_{\mathrm{rev}}(H_{\mathrm{a}}) = \frac{M_{\mathrm{sat}}}{H_{\mathrm{pen}}} \quad -H_0 < |H_{\mathrm{a}}| < H_0 < H_{\mathrm{pen}}, \tag{20}$$

(b) When $H_0 > H_{\mathrm{pen}}$,

$$M_{\mathrm{rev}} = M_{\mathrm{sat}}\left(1 - \frac{H_0}{H_{\mathrm{pen}}} + \frac{H_{\mathrm{a}}}{H_{\mathrm{pen}}}\right) \quad H_{\mathrm{a}} > H_0 - 2H_{\mathrm{pen}}, \tag{21}$$

$$M_{\mathrm{rev}} = -M_{\mathrm{sat}} \quad H_{\mathrm{a}} < H_0 - 2H_{\mathrm{pen}}. \tag{22}$$

Using Eqs. (14) and (15), we obtain

$$\chi'(H_0) = \frac{M_{\mathrm{sat}}}{H_{\mathrm{pen}}} \quad H_0 < H_{\mathrm{pen}}, \tag{23}$$

$$\chi'(H_0) = \frac{M_{\mathrm{sat}}}{H_{\mathrm{pen}}}\left[\frac{1}{2} - \frac{1}{\pi}\arcsin\left(1 - \frac{2H_{\mathrm{pen}}}{H_0}\right) - \frac{1}{\pi}\left(1 - \frac{2H_{\mathrm{pen}}}{H_0}\right)\sqrt{1 - \left(1 - \frac{2H_{\mathrm{pen}}}{H_0}\right)^2}\right] \quad H_0 > H_{\mathrm{pen}} \tag{24}$$

and

$$\chi''(H_0) = 0 \quad H_0 < H_{\mathrm{pen}}, \tag{25}$$

$$\chi''(H_0) = \frac{4M_{\mathrm{sat}}}{\pi H_{\mathrm{pen}}}\left(\left[\frac{H_{\mathrm{pen}}}{H_0}\right]^2 - \frac{H_{\mathrm{pen}}}{H_0}\right) \quad H_0 > H_{\mathrm{pen}}. \tag{26}$$

We observe that all the curves collapse into a single curve when normalizing the susceptibility to the initial susceptibility value $\chi_0 = M_{\mathrm{sat}}/H_{\mathrm{pen}}$ and the amplitude of the ac field H_0 to H_{pen}.

We can analytically obtain from the simple model the limiting curves for the case $H_0 \gg H_{\mathrm{pen}}$ as

$$\chi'(H_0 \gg H_{\mathrm{pen}}) = \frac{2}{\pi}\left(-\sqrt{\frac{H_{\mathrm{pen}}}{H_0}} - \frac{H_{\mathrm{pen}}}{H_0}\right) + \mathcal{O}(H_{\mathrm{pen}}/H_0)^{3/2}, \tag{27}$$

$$\chi''(H_0 \gg H_{\mathrm{pen}}) \simeq \frac{4}{\pi}\left(-\frac{M_{\mathrm{sat}}}{H_0}\right). \tag{28}$$

C. Results

In Figs. 6(a) and 6(b) we plot the calculated magnetization loops for different γ and δ values. The magnetization of a superconducting ring has the peculiarity that, for some of the geometrical parameters, it presents a kink. It can be observed that these kinks are easily distinguishable for $\delta > \simeq 0.5$ and all γ's. The kink is more evident for large δ's. The field at which the kink is produced is, exactly, the penetration field, in all cases, as long as J_c is considered constant. We observe that the initial slope of the magnetization curve increases (in magnitude) with decreasing γ because of the demagnetization effects, as known for cylinders.[12] The slope increases (in magnitude) with increasing the value of δ as well, so that narrower rings have larger initial slope, $\chi_{\mathrm{ini}} = \lim_{H_{\mathrm{a}} \to 0}(M_z/H_{\mathrm{a}})$. This effect is not due to the increase of the demagnetization effects when δ is larger. Instead the reason is that the saturation magnetization of a ring is larger than that for a bulk cylinder with the same γ [Eq. (9)]. Moreover, the penetration field is smaller as δ increase [Eq. (2) and Fig. 3]. As a consequence, the initial slope should be larger in magnitude.

In Fig. 7 we present the real and imaginary susceptibility calculated from the values of magnetization for different values of γ and $\delta = 0.8$, together with the expressions coming from the simple analytical model [Eqs. (21)–(24)]. A kink in both components of the susceptibility is observed, consistent with experimental results on actual YBCO rings.[20,30] This kink is a consequence of the one appearing in the magnetization loop, produced when the amplitude of the applied field equals the full penetration field. Therefore, same as for the magnetization loops, the kink is more evident for small γ's and large δ's. Thus, the measurements of magnetization or susceptibility in rings can be used to find the full penetration field from the kink as well, from which, using Eq. (2), the critical-current density can be obtained.

IV. CONCLUSIONS

We have studied the penetration of currents inside a finite superconducting ring, based on the critical-state model with constant critical current density J_c. The value of J_c of a superconductor can be obtained directly from the measurement of the magnetic field at one point. This is because the presence of the hole in the ring produces a sharp change in the process of penetration of currents inside the superconductor which is translated to a kink in the total field versus applied field as well as in the magnetization loops and the susceptibility curves. This kink is produced just when the superconducting sample becomes fully penetrated. The dependence of

this field upon the sample geometry can be obtained from an approximate expression [Eq. (2)], therefore providing a useful technique to determine J_c. The kink is more evident for thin and narrow rings, being therefore this geometry an optimum candidate for determining J_c of a superconducting sample.

The model developed for rings can be easily extended to the case of cylindrical superconductors composed of different coaxial cylindrical tubes.

ACKNOWLEDGMENTS

This work has been supported by Spain's Ministerio de Educación y Ciencia (FIS2004-02792) and Generalitat de Catalunya (SGR 2001-00189 and CeRMAE).

[1] C. P. Bean, Rev. Mod. Phys. **36**, 31 (1964).
[2] W. A. Fietz and W. W. Webb, Phys. Rev. **178**, 178 (1969).
[3] D.-X. Chen and R. B. Goldfarb, J. Appl. Phys. **66**, 2849 (1989).
[4] P. Chaddah, K. W. Bhagwat, and G. Ravikumar, Physica C **159**, 570 (1989).
[5] T. H. Johansen and H. Bratsberg, J. Appl. Phys. **77**, 3945 (1995).
[6] A. Sanchez and C. Navau, Supercond. Sci. Technol. **14**, 444 (2001).
[7] M. Pannetier, F. C. Klaassen, R. J. Wijngaarden, M. Welling, K. Heeck, J. M. Huijbregtse, B. Dam, and R. Griessen, Phys. Rev. B **64**, 144505 (2001).
[8] A. Forkl, Phys. Scr., T **T49**, 148 (1993).
[9] E. Pardo, A. Sanchez, and C. Navau, Phys. Rev. B **67**, 104517 (2003).
[10] A. Sanchez and C. Navau, Phys. Rev. B **64**, 214506 (2001).
[11] L. Prigozhin, J. Comput. Phys. **144**, 180 (1998).
[12] K. V. Bhagwat and P. Chaddah, Physica C **190**, 444 (1992)
[13] E. H. Brandt, M. Indebom, and A. Forkl, Europhys. Lett. **22**, 735 (1993).
[14] J. R. Hull, Supercond. Sci. Technol. **13**, R1 (2000)
[15] M. Tomita and M. Murakami, Nature (London) **421**, 517 (2003).
[16] A. B. Surzhenko, M. Zeisberger, T. Habisreuther, W. Gawalek, and L. S. Uspenskaya, Phys. Rev. B **68**, 064504 (2003).
[17] H. Claus, U. Welp, H. Zheng, L. Chen, A. P. Paulikas, B. W. Veal, K. E. Gray, and G. W. Crabtree, Phys. Rev. B **64**, 144507 (2001).
[18] H. Ohsaki, T. Shimosaki, and N. Nozawa, Supercond. Sci. Technol. **15**, 754 (2002).
[19] H. Teshima, T. Tawara, J. Kobuchi, T. Suzuki, and R. Shimada, *IEEE (PCC-Nagaoka'97)*, 1997; p. 701.
[20] T. Herzog. H. A. Radovan, P. Ziemann, and E. H. Brandt, Phys. Rev. B **56**, 2871 (1997).
[21] F. M. Araujo-Moreira, C. Navau, and A. Sanchez, Phys. Rev. B **61**, 634 (2000).
[22] C. Navau and A. Sanchez, Phys. Rev. B **64**, 214507 (2001).
[23] C. Navau and A. Sanchez, Supercond. Sci. Technol. **15**, 1445 (2002).
[24] E. H. Brandt, Phys. Rev. B **58**, 6506 (1998).
[25] Actually, what are calculated are the contour lines of $rA_\phi(r,z)$ at nonequidistant levels $rA_\phi = k\left(\nu - \frac{1}{2}\right)\left|\nu - \frac{1}{2}\right|$ (being k a constant and $\nu = 0, 1, 2, \ldots$). The value A_ϕ is the angular component of the vector potential created by both the currents and the applied field. Although these lines are not exactly the field lines, they are directed along the direction of the total field and they are equidistant when **H** is constant, with line density proportional to the field strength H (see Ref. 26).
[26] X. Granados, S. Sena, E. Bartolomé, A. Palau, T. Puig, X. Obradors, M. Carrera, J. Amorós, and H. Claus, IEEE Trans. Appl. Supercond. **13**, 3667 (2003).
[27] M. Carrera, J. Amorós, X. Obradors, and J. Fontcuberta, Supercond. Sci. Technol. **16**, 1187 (2003).
[28] J. R. Clem and A. Sanchez, Phys. Rev. B **50**, 9355 (1994).
[29] E. H. Brandt, Phys. Rev. B **55**, 14513 (1997).
[30] F. Mrowka, M. Wurlitzer, P. Esquinez, E. H. Brandt, M. Lorentz, and K. Zimer, Appl. Supercond. Lett. **70**, 898 (1997).